

# Bifurcation of an Inductively Coupled Josephson Junction Circuit

Tetsushi UETA<sup>†</sup> and Hiroshi KAWAKAMI<sup>†</sup>, Members

**SUMMARY** Some qualitative properties of an inductively coupled circuit containing two Josephson junction elements with a dc source are investigated. The system is described by a four-dimensional autonomous differential equation. However, the phase space can be regarded as  $S^1 \times \mathbf{R}^3$  because the system has a periodicity for the invariant transformation. In this paper, we study the properties of periodic solutions winding around  $S^1$  as a bifurcation problem. Firstly, we analyze equilibria in this system. The bifurcation diagram of equilibria and its topological classification are given. Secondly, the bifurcation diagram of the periodic solutions winding around  $S^1$  are calculated by using a suitable Poincaré mapping, and some properties of periodic solutions are discussed. From these analyses, we clarify that a periodic solution so-called "caterpillar solution" [1] is observed when the two Josephson junction circuits are weakly coupled.

**key words:** Josephson junction, bifurcation, caterpillar solution

## 1. Introduction

The motivation of this research is to clarify the mechanism of physical rotational systems; damped pendulum, phase-locked loop, robot arms, and so on. In such systems, there are various nonlinear phenomena due to the trigonometric characteristics of the state variable.

Since current-flux characteristics of a Josephson junction (JJ) element is given by a sinusoidal curve, a circuit containing some JJ elements and other linear elements can be regarded as rotational dynamical system. For example, a parallel circuit of a JJ element and a linear inductor is equivalent to a damped pendulum with elastic restoring force. We found previously that there are many types of heteroclinic orbits in the circuit [2].

In this paper, we treat an inductively coupled circuit containing two JJ elements with a dc source. The system is described by four-dimensional autonomous differential equation, however, the phase space can be regarded as  $S^1 \times \mathbf{R}^3$  because the system has a periodicity for the invariant transformation. We study the properties of periodic solutions winding around  $S^1$  as a bifurcation problem.

Firstly, we analyze equilibria in this system. The bifurcation diagram of equilibria and its topological classification are given. Secondly, the bifurcation diagrams of the periodic solutions winding around  $S^1$  are calculated by using a suitable Poincaré mapping, and

properties of periodic solutions are discussed. In particular, we clarify that a periodic solution so-called "caterpillar solution" [1] is observed when the two Josephson junction circuits are weakly coupled.

## 2. The Circuit Model

Figure 1 shows an inductively coupled circuit containing two JJ elements with the same characteristics. This circuit is equivalent to a SQUID (superconducting quantum interference device) containing two junctions. The characteristics of a JJ element are assumed as:

$$i_J = I_c \sin \phi_i, \quad \frac{d\phi_i}{dt} = \frac{2e}{\hbar} v_i \quad i = 1, 2. \quad (1)$$

where,  $I_c$ ,  $e$ ,  $\hbar$  are the critical current of a JJ element, the charge of electron, and Planck's constant, respectively.  $\phi$  is the phase difference of the wave function at the center of the junction plane.

To normalize circuit equations, we introduce the following new parameters and variables:

$$\begin{aligned} k &= \sqrt{\frac{\hbar}{2eI_c C}} G \\ c &= \frac{\hbar}{2eI_c L} \\ B_0 &= \frac{J}{I_c} \\ \tau &= \sqrt{\frac{2eI_c}{\hbar C}} t \\ x_i &= \phi_i \\ y_i &= \sqrt{\frac{2eC}{\hbar I_c}} v_i, \end{aligned} \quad (2)$$

where,  $i = 1, 2$ . For simplicity, we assume that  $G$  is a linear conductance. If we rewrite  $\tau$  as  $t$ , we obtain the following four-dimensional autonomous differential equations:

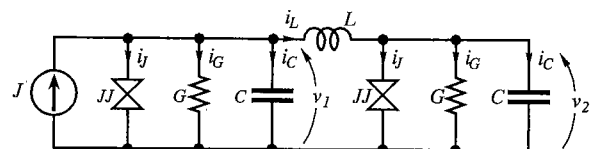


**Fig. 1** The circuit with two Josephson junction elements coupled by inductance  $L$ .

Manuscript received February 24, 1994.

Manuscript revised May 9, 1994.

<sup>†</sup>The authors are with Faculty of Engineering, The University of Tokushima, Tokushima-shi, 770 Japan.

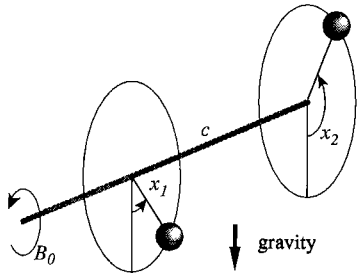


**Fig. 2** Physical interpretation of the system (3). Both terminals of the joint are free.

$$\begin{aligned} \frac{dx_1}{dt} &= y_1 \\ \frac{dy_1}{dt} &= -ky_1 - \sin x_1 - c(x_1 - x_2) + B_0 \\ \frac{dx_2}{dt} &= y_2 \\ \frac{dy_2}{dt} &= -ky_2 - \sin x_2 - c(x_2 - x_1). \end{aligned} \tag{3}$$

The system (3) is equivalent to a parallel pendula connected by an elastic torsional joint with the gravity force. Therefore,  $k$  is interpreted as a coefficient of damping,  $c$  as an elasticity constant, and  $B_0$  as an external torque. See Fig. 2.

### 3. Properties of the System

#### 3.1 Invariance

Equations (3) are invariant for the transformation:

$$(x_1, y_1, x_2, y_2) \rightarrow (x_1 + 2n\pi, y_1, x_2 + 2n\pi, y_2), \tag{4}$$

where,  $n$  is an integer. Note that  $x_1$ , and  $x_2$  cannot be taken modulo  $2\pi$  individually, but  $x_1 + x_2$  can be. Hence state space of this system can be considered as  $S^1 \times \mathbf{R}^3$ . To visualize a circle  $S^1$  in  $x_1$ - $x_2$  plane, a new coordinate  $(u, v)$  is introduced as follows:

$$u = \frac{1}{2}(x_1 + x_2), \quad v = \frac{1}{2}(x_1 - x_2). \tag{5}$$

From Eqs. (4) and (5), we can find  $S^1$  as the semi-open interval  $[0, 2\pi)$  on  $u$  without information of  $y_1$  and  $y_2$ . This transformation is useful to analyze periodic solutions discussed in Sect. 5

#### 3.2 Boundedness

The mechanical energy of Eqs. (3) is follows:

$$\begin{aligned} E &= \frac{1}{2}(y_1^2 + y_2^2) - \cos x_1 - \cos x_2 \\ &\quad - B_0 x_1 + \frac{1}{2}c(x_1 - x_2)^2. \end{aligned} \tag{6}$$

Any solution of Eqs. (3) is bounded because  $dE/dt$  is negative for  $k > 0$ . This also shows that there is

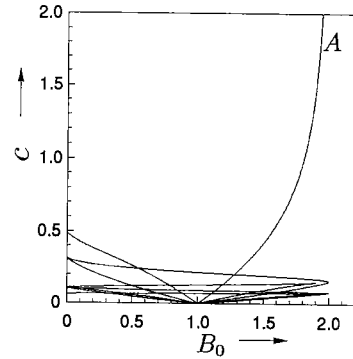


**Fig. 3** The bifurcation diagram of equilibria of Eqs. (3).

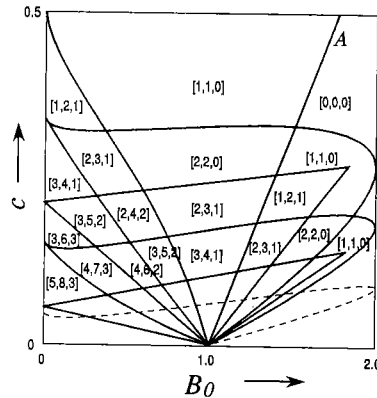


**Fig. 4** Illustration of bifurcation diagram Fig. 3. Any sequence means  $[\#\{0O\}, \#\{1O\}, \#\{2O\}]$ .

no periodic solution homotopic to an equilibrium [3]. Thus, there exists a finite set  $M$  in the  $\mathbf{R}^4$ , and any orbit started from arbitrary initial condition enters to  $M$  until infinite time eventually, and it is captured by a stable equilibrium, or a solution winding around cylinder.

### 4. Classification of Equilibria

Equilibria of (3) are calculated by solving equations:

$$f(x_2) = \sin\left(\frac{1}{c} \sin x_2 + x_2\right) + \sin x_2 = B_0 \tag{7}$$

$$x_1 = x_2 + \frac{1}{c} \sin x_2. \tag{8}$$

Note that  $f(x_2)$  is a periodic function with period  $2\pi$ . Thus tangent (saddle-node) bifurcations for equilibria can be calculated at  $df(x_2)/dx_2 = 0$  in  $0 \leq x < 2\pi$ . Figure 3 shows the bifurcation diagram of equilibria.

Topological properties of an equilibrium is determined by roots of the characteristic equation corresponding to the Jacobi matrix with respect to Eqs. (3). Using Routh-like criterion of stabilities, the topological classification of equilibria is achieved in  $B_0$ - $c$  plane. Figure 4 is illustration of Fig. 3 for  $c < 0.5$  with topological classification of equilibria.

The following properties are found in Figs. 3 and 4:

1. In each region surrounded by bifurcation curves, the number of equilibria is invariant.
2. For  $k > 0$ , we have only three types of equilibria:  ${}_0O$ (completely stable),  ${}_1O$ (1-dimensionally unstable),  ${}_2O$ (2-dimensionally unstable). Other types which are possible combinations;  ${}_3O$ (3-dimensionally unstable) and  ${}_4O$ (completely unstable), can not exist in the system.  ${}_1O$  means that either of the pendula is in an unstable equilibrium. In Fig. 4, we indicate the number of each type of equilibria by  $[\#\{{}_0O\}, \#\{{}_1O\}, \#\{{}_2O\}]$ .  $\#\{\}$  indicates the number of elements contained in the set  $\{\}$ .
3. When parameters vary across any bifurcation curves,  $\#\{{}_1O\}$  changes by 1, and either of  $\#\{{}_2O\}$  and  $\#\{{}_0O\}$  changes by 1.
4.  $B_0 = 2.0$  is an asymptotic line for bifurcation curve labeled by  $A$ , because Eq. (7) tends to  $2 \sin x_2 = B_0$  as  $c \rightarrow \infty$ . In the circuit model,  $c \rightarrow \infty$  means  $L \rightarrow 0$ . Then this is reduced to the circuit containing a single JJ element with dc source or the damped pendulum with constant torque.
5. When any parameter moves from  $[1, 1, 0]$  region to  $[0, 0, 0]$  region, all equilibria are disappeared. From the boundedness discussed in Sect. 3.2, we can observe that the orbit captured by this equilibrium begins to move and tends asymptotically toward a limit cycle (periodic solution winding around  $S^1$ ).
6. As  $c \rightarrow 0$ , many equilibria appear. Accordingly, orbits started from any initial state tend to behave independently. Just at  $c = 0$ , the equilibrium converges to  $(x_1, x_2) = (\sin^{-1}B_0, 0)$ , then the system (3) is split into two completely independent second-order system  $(x_1, y_1), (x_2, y_2)$ .

**5. Bifurcation of Periodic Solutions**

In this section, we show the bifurcation diagram to explain properties of periodic solutions of Eqs. (3).

**5.1 Poincaré Mapping**

In order to discuss the properties of periodic solutions and their bifurcations, we define the following Poincaré mapping.

For simplicity, let Eqs. (3) be rewritten as:

$$\frac{dx}{dt} = f(x, \lambda) \tag{9}$$

where,  $x = \{x_1, y_1, x_2, y_2\}$ ,  $\lambda = \{k, c, B_0\}$ . We denoted also the solution of Eq. (9) with the initial value  $x_0$  at  $t = 0$  as:

$$x(t) = \varphi(t, x_0), \quad x(0) = \varphi(0, x_0) = x_0. \tag{10}$$

Suppose that we have a periodic solution as:

$$x(t) = \varphi(t, \hat{x}). \tag{11}$$

We can choose a hyperplane  $\Pi$  through  $\hat{x} \in \mathbf{R}^4$  transverse to the solution of Eq. (9). For each point  $x \in U$ , a small neighborhood of  $\hat{x}$  in  $\Pi$ , the solution  $\varphi(t, x)$  will intersect  $\Pi$  after a finite time  $\tau$ , i.e.,

$$\varphi(\tau, x) = x_\tau \in \Pi \tag{12}$$

Hence we define a mapping  $T_\lambda$  called a Poincaré mapping from  $U$  into  $\Pi$  as:

$$T_\lambda : \Pi \supset U \rightarrow \Pi \\ x \mapsto x_\tau = \varphi(\tau, x) \tag{13}$$

Note that the return time  $\tau$  depends on the initial value  $x \in U$ . For Eqs. (3), we can consider  $\Pi$  as:

$$\Pi = \{x \in \mathbf{R}^4 : x_1 + x_2 = 0\} \tag{14}$$

from the property of the transformation (4), however,

$$\Pi = \{x \in \mathbf{R}^4 : x_1 = 0\} \tag{15}$$

is chosen for the convenience of taking modulo  $2\pi$  for  $x_1$  and  $x_2$ . Thus, we can calculate the bifurcation values of the parameters using by  $T_\lambda$  and its derivative  $DT_\lambda$ . In the following, system parameter  $k$  is fixed at 0.2.

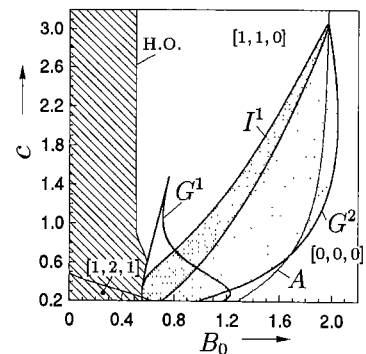
**5.2 Bifurcation Diagram**

Figure 5 shows a bifurcation diagram of periodic solutions. For simplicity, we studied  $c > 0.2$  mainly because this plane is almost covered by  $[1, 1, 0]$  region containing two equilibria; a sink and a saddle.

We observed two types of bifurcation in this system; local bifurcations and global bifurcations. The former are tangent bifurcation and period doubling bifurcation for periodic solutions, and the latter is the homoclinic bifurcation for the trajectory.

The following properties are found in Fig. 5.

1. In the white region, there exists a periodic solu-



**Fig. 5** Bifurcation diagram of periodic solutions.  $k = 0.2$ .

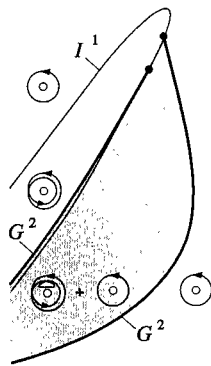


Fig. 6 Magnification of Fig. 5.

tion corresponding to a fixed point of  $T_\lambda$ . This synchronous solution has constant and positive velocities with a small phase shift. See Fig. 7 (b).

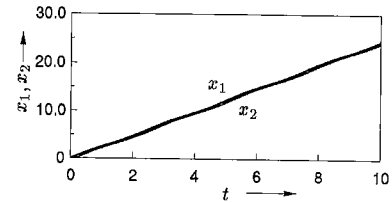
2.  $I^1$  shaping the dark shaded island is a period doubling bifurcation curve for the fixed point.
3.  $G^2$  indicating the tangent bifurcation curve for the 2-periodic point is connected to  $I^1$  curve. See Fig. 6. The 2-periodic point bifurcated from the upper portion of  $I^1$  disappears by the lower portion of  $G^2$ .
4.  $G^1$  is the tangent bifurcation curve for the fixed points. In the region surrounded by this curve, there exist two stable fixed points.
5. The line labeled by 'H.O.' indicates homoclinic orbit meaning global bifurcation, i.e., a periodic orbit and a separatrix loop for  $1O$  coalesce at this parameter. Thus there is no periodic solution in hatched region.

### 5.3 The Caterpillar Solution

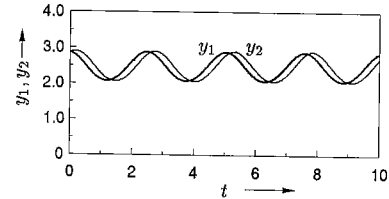
We observe a periodic solution called "caterpillar solution" defined by Levi [1] as a periodic points for  $T_\lambda$ . We recall the definition of the caterpillar solution from Ref. [1]:

**Definition:** (Levi) A periodic solution  $\varphi = (\varphi, \dot{\varphi}, \psi, \dot{\psi})$  of Eqs. (3) is called a caterpillar solution if its period consists of two intervals during the first of which  $\varphi$  increases by  $2m\pi + R_1$ ,  $m$  being an integer and  $0 < R_1 < \pi/2$ , while  $\psi$  changes by less than  $\pi/2$ ; during the second time interval  $\varphi$  and  $\psi$  exchange roles:  $\psi$  increases by  $2m\pi + R_2$  and  $\varphi$  changes by less than  $\pi/2$ .

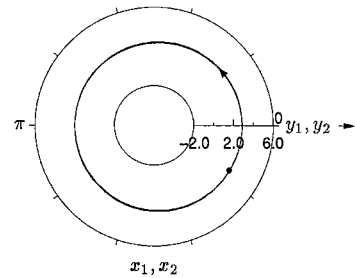
This definition gives only the quantity corresponding to its wave form, however, to calculate accurate region satisfying the definition is not our goal. We assert that bifurcations for the periodic solutions are the essential reason why the caterpillar solution is involved. In practical, if the distance between upper and lower



(a)



(b)



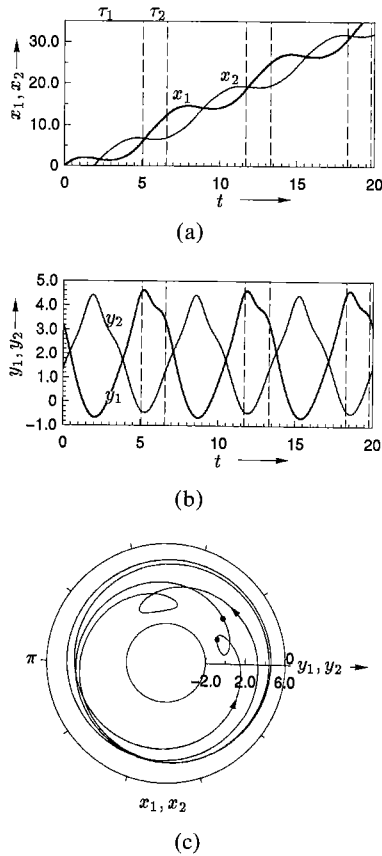
(c)

Fig. 7 Time response of periodic solution with fixed point for  $T_\lambda$ . (a) States, (b) Velocities, (c) Cylindrical phase portrait. A circled point indicate a periodic point.  $c = 1.2$ ,  $B_0 = 1.0$ ,  $\tau = 2.503$ .

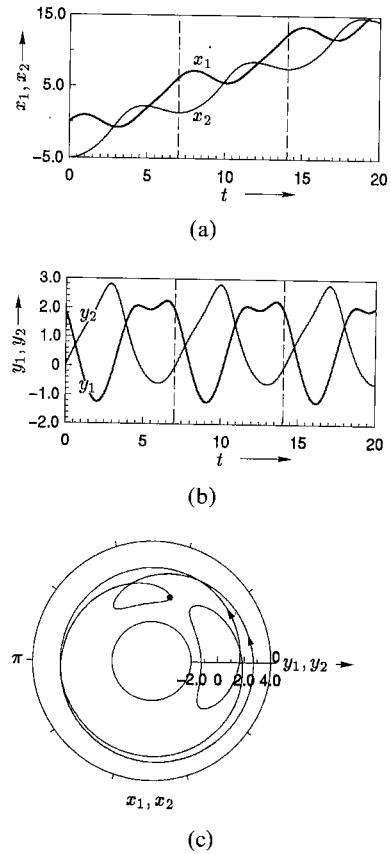
$G^2$  curves is separated sufficiently, then the wave form of 2-periodic points bifurcated by  $I^1$  is distorted as  $c$  tends to 0. See property 6 in Sect. 4

Figure 8 shows a caterpillar solution.  $\tau_1$  and  $\tau_2$  are periods for Poincaré mapping. Note that velocities  $y_1$  and  $y_2$  can be observed as the almost out-of-phase synchronous motions. To obtain another explanation for caterpillar solutions, we observe the motion of orbits in  $x_1$ - $x_2$  plane. Figure 9 illustrates the coordinate introduced by Eq. (5) containing a circular space  $S^1$  on  $u$ . The period of the orbit corresponds to the number of black circles indicating intersectional points of the orbit and  $v$ -axis using by Poincaré section (14). In this figure, two orbits with 2-periodic points are drawn. (a) is an orbit whose periodic points are located nearly on  $v$ . This orbit is just branched by  $I^1$  in Fig. 5 and runs almost parallel to the coordinate  $u$ . The orbit (b) considered as a caterpillar solution whose parameters are equal to the solution drawn in Fig. 8 and which is transmuted from (a) as  $c$  decreases. It is clear that the caterpillar solution moves like a step function for the coordinate  $x_1$  or  $x_2$ .

In Fig. 6, the periodic solution bifurcated by  $G^1$  also can be regarded as a caterpillar solution. See Fig. 10. In  $c < 0.5$ , therefore, we conclude that bifur-



**Fig. 8** Time response of 2-periodic caterpillar solution. (a) States, (b) Velocities, (c) Cylindrical phase portrait. A circled point indicates a periodic point.  $c = 0.48$ ,  $B_0 = 1.36$ ,  $\tau_1 = 5.056$ ,  $\tau_2 = 1.5217$ .



**Fig. 10** Time response of periodic solutions with fixed point.  $c = 0.4$ ,  $B_0 = 1.0$ ,  $\tau = 7.0195$ .

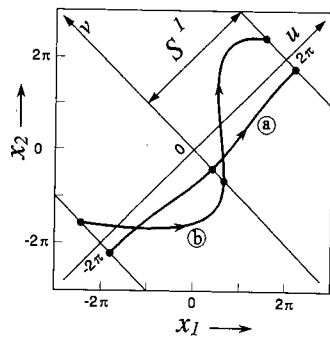


**Fig. 9** Two types of 2-periodic orbits in  $x_1$ - $x_2$  plane.

cations for a periodic solution and small value of  $c$  are closely related to the generation of caterpillar solutions.

5.4 Other Solutions

There are so many bifurcation curves and periodic solutions in the region surrounded by  $I^1$ ,  $G^1$  and  $G^2$ . Some of these periodic solutions satisfy the condition of caterpillar solution.

Figure 11 shows a chaotic solution caused by a pe-

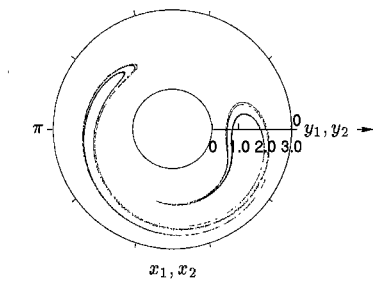


**Fig. 11** Chaotic solution.  $c = 0.48$ ,  $B_0 = 0.86$ .

riod doubling cascade, but this solution does not satisfy the definition of the caterpillar solution.

6. Concluding Remarks

In this paper, properties for equilibria and periodic solutions observed in the inductively coupled JJ circuit are investigated and their bifurcation diagram are obtained. Firstly, the parameter region in which equilibria exist is given. We clarify that the topological properties of equilibria using by the bifurcation diagram and suitable classifications. Secondly, the bifurcation diagram of periodic solutions winding around  $S^1$  are obtained. This

explains some properties of periodic solutions. Particularly, it is clear that the caterpillar solution are caused by a small parameter  $c$  and bifurcations.

Further study is needed to obtain a detailed bifurcation diagram for  $c < 0.2$ . Moreover, investigations of the properties of the circuit in non-autonomous system and a circuit with JJ elements coupled by a resistor are future objectives of research.

### Acknowledgment

The authors would like to thank the reviewers for their valuable comments and suggestions.

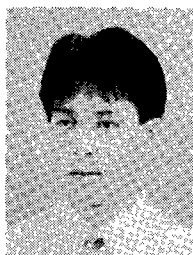
### References

- [1] Levi, M., "Beating Modes in the Josephson Junction," In US Army Research Office, *Chaos in Nonlinear Dynamical Systems*, pp.56-73, SIAM, 1984.
- [2] Ueta, T. and Kawakami, H., "Bifurcation of Heteroclinic Orbits in a Circuit Containing A Josephson Junction Element," *Trans. IEICE*, vol.J76-A, no.10, pp.1450-1456, Oct. 1993.
- [3] Kawakami, H., "Qualitative Properties of Forced Oscillations on the Cylindrical Phase Surface," *Trans. IEICE*, vol.J64-A, no.11, pp.916-923, 1981.
- [4] Kawakami, H., "Bifurcation of Periodic Responses in Forced Dynamic Nonlinear Circuits: Computation of Bifurcation Values of the System Parameters," *IEEE Trans. Circuits & Syst.*, vol.CAS-31, pp.248-260, 1984.
- [5] Yoshinaga, T. and Kawakami, H., "Mode Bifurcations in Diffusively Coupled van der Pol Equations," *IEICE Trans.*, vol.E-74, no.6, pp.1420-1427, Jun. 1991.



**Hiroshi Kawakami** was born in Tokushima, Japan, on December 6, 1941. He received the B.Eng. degree from Tokushima University, Tokushima, Japan, in 1964, the M.Eng. and Dr.Eng degrees from Kyoto University, Kyoto, Japan, in 1966 and 1974, respectively, all in electrical engineering. Presently, he is Professor of Electrical and Electronic Engineering, Tokushima University, Tokushima, Japan. His interest is qualitative properties of nonlinear circuits.

erties of nonlinear circuits.



**Tetsushi Ueta** was born in Kochi, Japan, on March 1, 1967. He received the B.Eng. in Electronic engineering, and M.Eng. in Electrical engineering from Tokushima University, in 1990, and 1992, respectively. Since 1992, he was been Research Associate of Information Science and Intelligent Systems, Tokushima University. His interest is bifurcation problems of dynamics.